Landslides (2023) 20:1679–1689
DOI 10.1007/s10346-023-02093-9
Received: 30 December 2022
Accepted: 19 May 2023
Published online: 5 June 2023

Zhichao Cheng · Shiqi Liu · Xuewen Fan · Anchi Shi · Kexin Yin

Deformation behavior and triggering mechanism of the Tuandigou landslide around the reservoir area of Baihetan hydropower station

Abstract The reservoir impoundment can lead to accelerated deformation or reactivation of landslides, posing great threats to human lives and dam stability. The primary objective of this paper is to report the movement process of the Tuandigou (TDG) ancient landslide in the Baihetan dam area during reservoir impounding. Field investigation, borehole work, and site monitoring data are used to analyze the deformation behavior and triggering mechanism of the TDG landslide. It is found that the landslide deformation is closely related to the reservoir water level. After the reservoir water level reached the elevation of 810 m on October 12, 2022, the ground cracks continued to expand and gradually linked up, resulting in an accelerated deformation of the TDG landslide. Furthermore, the lithology in the study area also positively contributes to the slide movement. Based on these results, it is anticipated that the present research will provide guidelines for the early warning and control of the TDG landslide during and after the reservoir impounding.

Keywords Landslide · Reservoir impounding · Deformation behavior · Triggering mechanism · Baihetan hydropower station

Introduction

The construction and impoundment of many large reservoirs in high and narrow valley areas can significantly change the hydrogeological condition of reservoir slopes and increase the frequency of geological hazards, particularly in the form of landslides (Paronuzzi et al. 2013; Tang et al. 2019; Wu et al. 2022; Yan et al. 2019; Zhou et al. 2022). These landslides induced by reservoir filling threaten human lives and dam stability (Huang et al. 2016; Wu et al. 2023; Yin et al. 2016). The best well-known example is the 1963 Vajont landslide in Italy, which led to about 270 million m^3 of sliding mass collapsing into the reservoir and generated an impulse wave 250 m above the original water level (Barla and Paronuzzi 2013; Crosta et al. 2015; Kilburn and Petley 2003; Wolter et al. 2015). Furthermore, villages nearby were destroyed, and more than 2000 people were killed (Ibañez and Hatzor 2018). A similar reservoir-induced geohazard is the Qianjiangping landslide, which occurred suddenly during the first impoundment of Three Gorges Reservoir in July 2003. It caused 24 deaths, the sinking of 22 fishing boats, and the direct economic loss of about 7 million US dollars (Tang et al. 2016; Wang et al. 2004, 2008; Yin et al. 2015). However, the prevention and early warning of landslides during and after reservoir filling are still challenging because of the complexity and randomness of trigger factors, such as topography, lithology, reservoir water level, rainfall, and earthquakes.

The Baihetan hydropower station on the lower reaches of the Jinsha River is the second largest hydropower station in China after the Three Gorges hydropower station. The first impoundment of the Baihetan reservoir began from a reservoir level of 657.55 m on April 6, 2021, and reached its normal water level of 825 m on October 25, 2022. Dun et al. (2021) used time-series InSAR technology to identify 21 active landslides between Hulukou and Xiangbiling within the Baihetan reservoir area before impoundment. They predicted that these potential landslides may slide after the reservoir filling. Indeed, the Wangjiashan ancient landslide underwent accelerated deformation during the first impoundment period, developing into overall sliding on 7 July 2021 (Liu et al. 2023; Yi et al. 2022). Landslides induced by reservoir impoundment have gradually become a contentious issue in the Baihetan reservoir.

Tuandigou (TDG) landslide is located on the left bank of the Jinsha River, which is approximately 22.5 km upstream from the Baihetan dam site. Further, the No. K8 + 465-K8 + 594 m section of the Dawanzi (DWZ) tunnel passes through the interior of the landslide. Since September 11, 2022, the reservoir water has increased rapidly, reaching its normal water level of 825 m on October 24, which is ultimately maintained at approximately 824 m. During the rapid rise of the reservoir water level, the deformation of the TDG landslide has accelerated since October 12, 2022. The stability of the landslide and its effect on the DWZ tunnel has raised huge concern among the authorities regarding the Baihetan reservoir region. Therefore, field investigation, borehole work, and displacement monitoring have been used to monitor the evolution process of the TDG landslide. The deformation characteristics and triggering mechanism have been analyzed and discussed based on the above multi-source data. The research presented in this paper can provide relevant guidance for the early warning and control of the TDG landslide during and after the filling period of the Baihetan reservoir.

Geological background of the Tuandigou landslide

Geological setting

TDG landslide is located on the left bank of the Jinsha River, which is approximately 22.5 km upstream from the Baihetan dam site. Both sides of the landslide are marked by $8^{\#}$ and $9^{\#}$ gully. Besides, the No. K8 + 465-K8 + 594 m section of DWZ tunnel passes through the interior of the landslide, as shown in Fig. 1. The TDG landslide has a chair-shaped morphology, with a gentle landform followed by a steep landform. The rear edge of the landslide at the elevation between 850 and 1300 m is slightly steep with slopes of 30–35°. The middle part of the landslide at 730–850 m elevation is steeper, with slope angles ranging from 40° to 45°. However, the slope angle is less than 15° at the front edge of the landslide below the 730 m elevation (Fig. 1a). The entire area of the TDG landslide is about 2.86,000 m^2

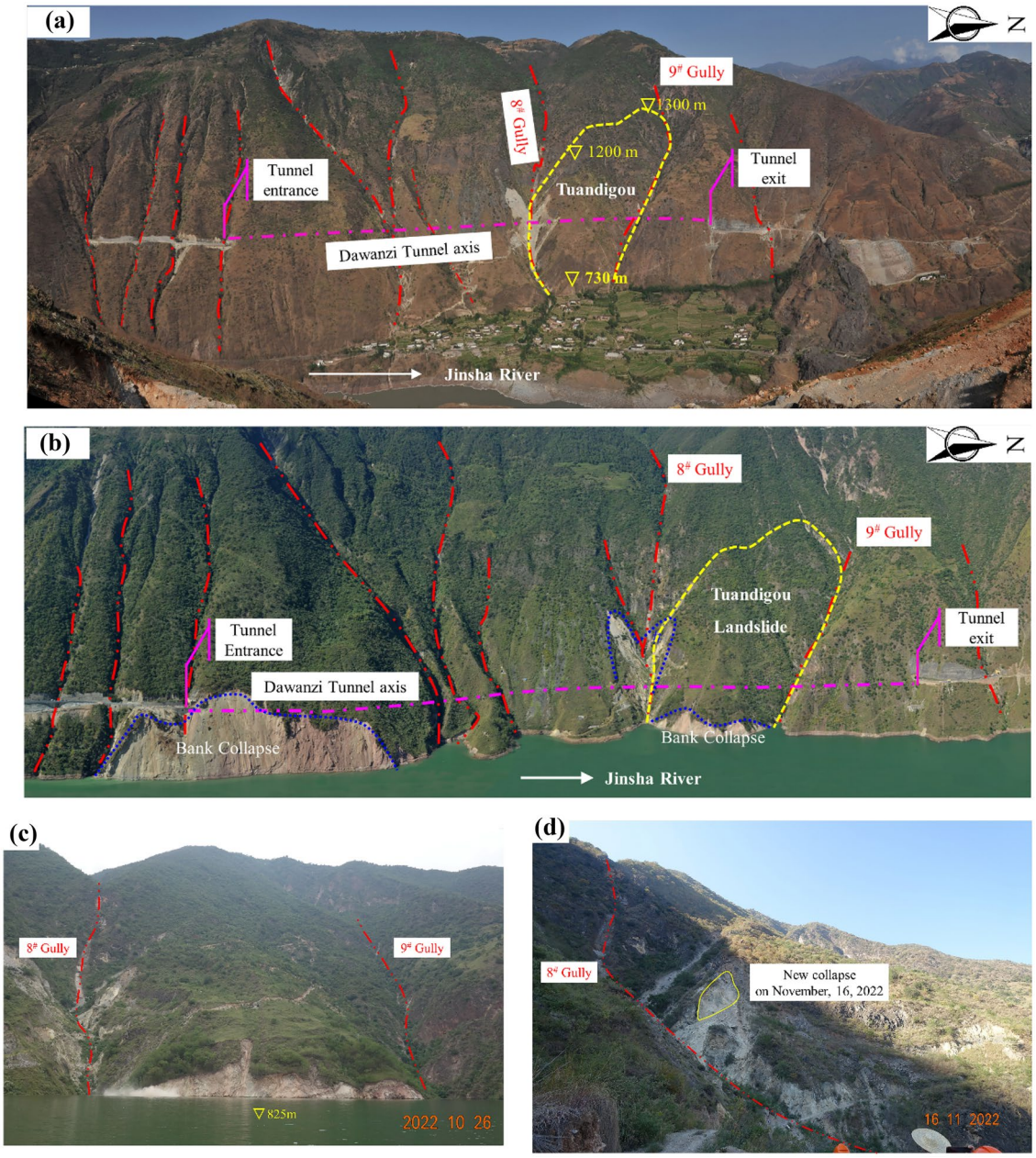

Fig. 1 Overview of Tuandigou landslide: **a** before the reservoir impounding, **b** after the reservoir impounding, **c** recent appearance of the TDG landslide, and **d** new collapse failure

with a longitudinal length of 800 m and a width of 358 m. The estimated volume of the landslide mass is approximately 19.82 million m^3, with an average thickness of 69.3 m.

From the geological point of view, the rock mass of TDG landslide is soft-weak at the elevation of 700–1300 m, and the bank slope is dip slop. Under the effect of gravity, the front edge of the rock mass gradually bends, resulting in tensile cracks in the bending zone. Moreover, due to weathering and unloading, the strength of the rock decreased, and the structural planes gradually extended and connected. During the cutting down of Jinsha River, the foot of the slope was located on the free face, ultimately leading to the collapse of the front edge and the shear failure of the rear edge along the bottom sliding surface, forming the relatively stable ancient TDG landslide. After the impoundment of the Baihetan reservoir, the reservoir water level rises rapidly, and the bank slope composed of collapsing rock mass is scoured by the reservoir water again. The rock mass at the front edge collapses, aggravating the deformation of the TDG landslide.

The study area belongs to the subtropical monsoon, with an annual average temperature ranging from 15 °C to 21 °C. The annual precipitation is about 600–1600 mm, and nearly 80% of the rainfall occurs in the rainy season between May and October each year. As shown in Fig. 2, the major faults crossing the study area are Daliangshan fault (F6), Zemuhe fault (F3), and Xiaojiang fault (F4).

The minimum distance from the TDG landslide to F6, F3, and F4 is approximately 1 km, 7 km, and 10 km, respectively. Based on the previous study of Liu et al. (2023), the F4 is the most active fault in the Baihetan reservoir area.

Material compositions and structure characteristics

The lithology and structural characteristics of the landslide are investigated by drilling and field surveys. A typical geological section of the TDG landslide is shown in Fig. 3. The uppermost covering layer is the Quaternary loose accumulation layer (Q). The bedrock outcropping in the study area is comprised of medium-thick dolomite from the Lower Cambrian layer (Є1), thin sandstone from the Middle Cambrian Xiwangmiao Formation layer (Є2x), and thin-medium dolomite from the Upper Cambrian Erdaoshui Formation layer (Є3e). The Є2x can be categorized into 4 layers (Є2 × 1–Є2 × 4) with a thickness of 25–30 m, 35–40 m, 8–10 m, and 170–190 m, respectively. The overall production of bedrock is NS/∠E45–55°. The drilling cores of ZK10, ZK11, and ZK12 reveal that the bottom sliding surface is composed of silty clay with gravel. The upper landslide mass mainly contains block stone and is partially mixed with fine-grained soil breccia.

Deformation characteristics of the landslide

In situ monitoring system

To better understand the deformation characteristics of the TDG landslide during the reservoir filling, field investigation, borehole work, and displacement monitoring are adopted by the hydropower plant authorities (Yi et al. 2022; Zhang et al. 2021). As shown in Figs. 4, 11 global navigation satellite system (GNSS) antennas and 4 borehole inclinometers are installed in the landslide area to measure the surface displacements and deep displacements, respectively. Most GNSS antennas are located in the range of landslide mass except for GNSS1 and GNSS11. The GNSS monitoring sites began on November 22, 2021, while the monitoring sites of borehole inclinometers started on September 14, 2022. Besides, the precipitation data of the TDG landslide and reservoir water level are also monitored, which will be used latter in our research.

Field investigation

Field investigations are carried out to identify the macroscopic deformation characteristics of the TDG landslide (Zhang et al. 2021). The main representation forms of deformation include the ground cracks and the damage to the DWZ tunnel.

As shown in Fig. 4, six typical tension cracks are formed and developed along the surface of the landslide. The deformation characteristics of ground cracks are illustrated in Fig. 5 and Table 1. It should be noted that cracks C1, C5, and C6 were discovered during the field investigation in October 2021, while cracks C2, C3, and C4 were found in April 2022 after comprehensive geological mapping of the landslide mass by excavating surveying and mapping sidewalks. The rear edge of the landslide is bounded by long and continuous developmental cracks C1 and C2, with a width of 20–40 cm, a dislocation of 40–50 cm, and a visible depth of more than 5 m.

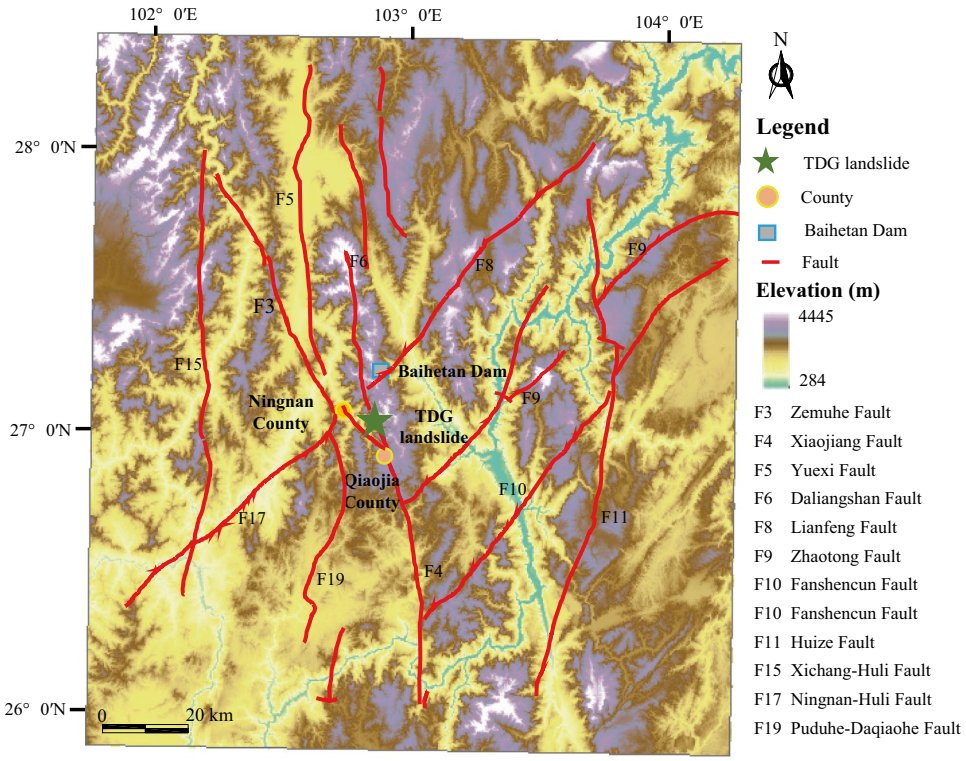

Fig. 2 Fault map of the area of TDG landslide

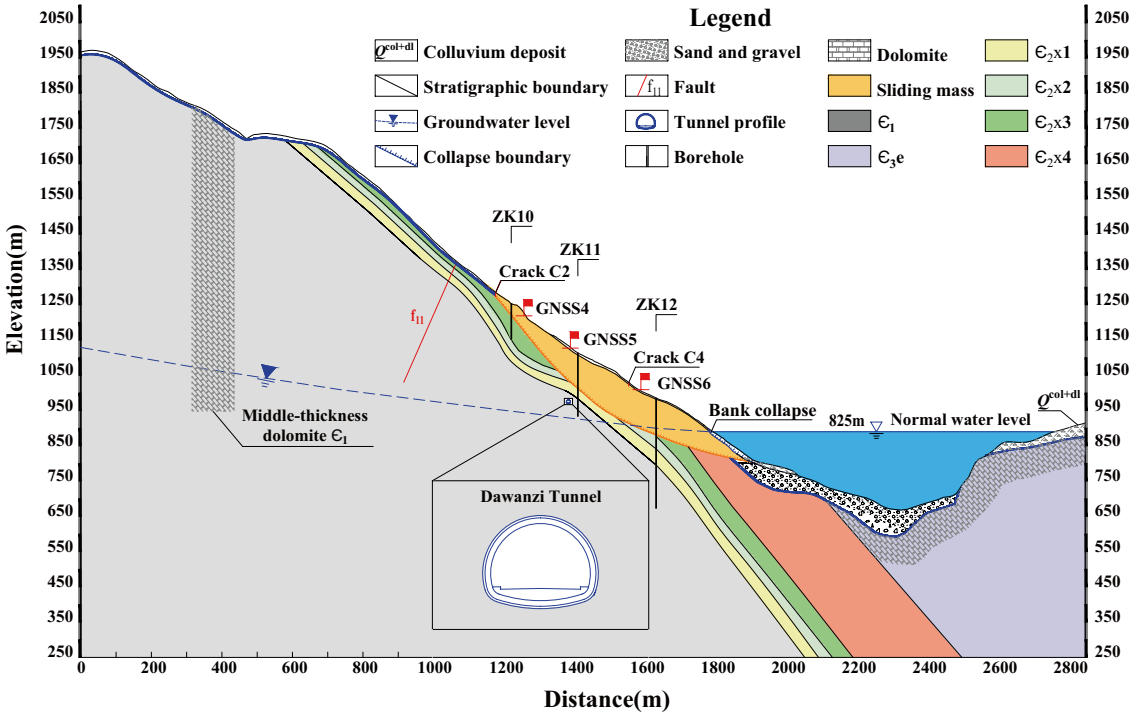

Fig. 3 Schematic geological cross-section map of TDG landslide

There are no rock fragments filling, weeds, and brush growing in all ground cracks. Therefore, the tension cracks observed on the landslide are generated after the reservoir's first impounding. After comparing with several field investigation, the width and dislocation of the tension cracks has been found to rapidly increase from April 2022 to October 2022. In addition, crack C4 is intermittently connected with crack C6, as shown in Fig. 6.

In addition, the DWZ tunnel in the section of K8 + 486–K8 + 548 m showed obvious rupturing and deformation. As shown in Fig. 7, the deformations which includes concrete cracking and local blocking

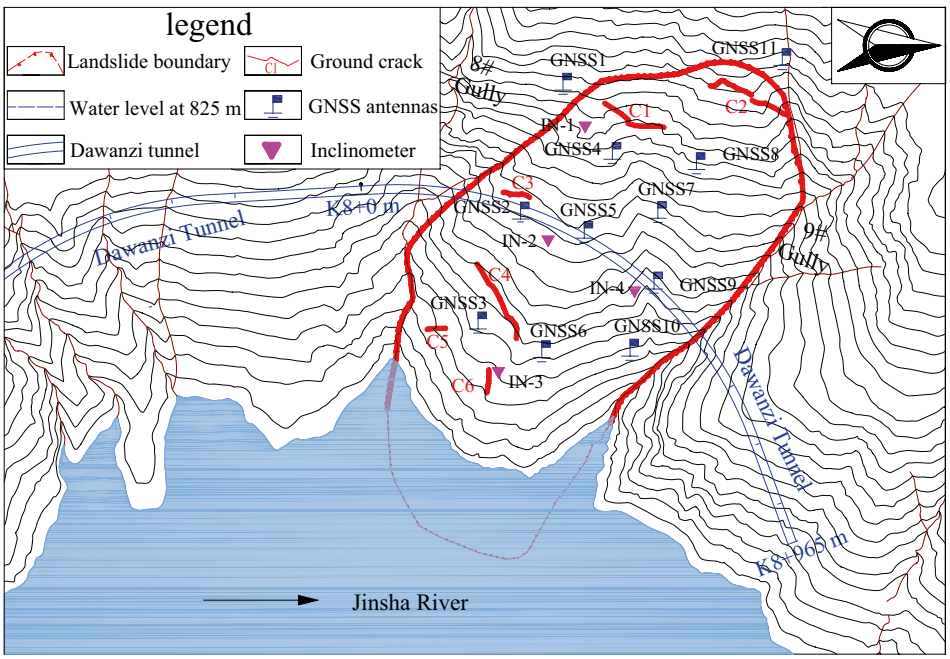

Fig. 4 Layout of the TDG landslide monitoring system

Fig. 5 Photos of typical cracks on the surface of the TDG landslide

Table 1 Summary of deformation characteristics of the main cracks

Crack name	Discovery time	Distributed elevation (m)	Description
C1	Oct. 2021	1170–1210	It is a tension crack at the rear edge of the landslide. As a whole, the crack extended in the direction of N23°E, with a length of 108 m, a width of 20–40 cm, a dislocation of 40–50 cm, and a depth of more than 5 m
C2	Apr. 2022	1195–1270	It is a tension crack at the rear edge of the landslide. The crack generally extended in the N23°E direction, with a length of 135 m, a width of 20–40 cm, a dislocation of 40–50 cm, and a depth of more than 5 m
C3	Apr. 2022	1070–1078	It is a tension crack in the middle of the landslide. In generally, the crack extended in the direction of N10°E. It is 45 m long, 20–30 cm wide, and 1–2 m deep
C4	Apr. 2022	958–975	It is a tension crack in the middle of the landslide. The crack extended in the direction of N62°E, with a length of 138 m, a width of 30–40 cm, and a depth of more than 3 m
C5	Oct. 2021	882–908	It is a tension crack in the front of the landslide, closed to the 8# gully. The crack extended in the direction of N15°W–N15°E, with a length of 29 m, a width of 10 cm, and a depth of more than 3 m
C6	Oct. 2021	905–930	It is a tension crack in the front of the landslide. It extended in the direction of N80°E. The crack is 28 m long, 20–30 cm wide, and more than 3 m deep

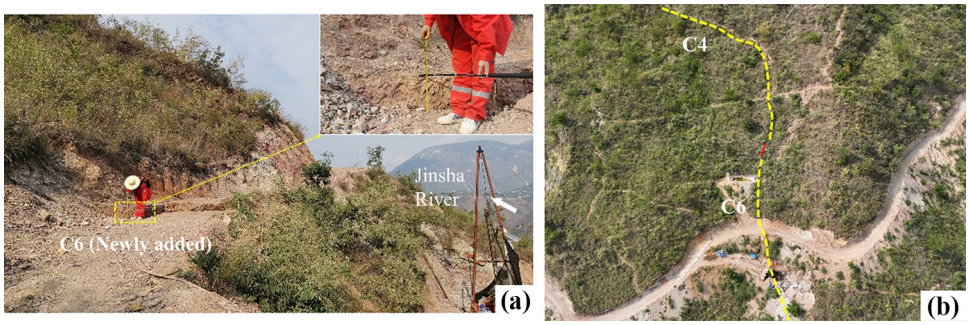

Fig. 6 Aggravated deformation characteristics of the cracks during the impounding

have been significantly aggravated since October 17, 2022. In the meantime, the water level of Baihetan reservoir fluctuated from 810 to 825 m. Currently, the water level is near the normal water level of 825 m, and the rate of fracture deformation is relatively large, showing no signs of slowing down.

Monitoring results

From November 2021 to September 2022, the reservoir water level fluctuated from 775.21 m to 800.21 m. Since September 11, 2022, the reservoir water has increased rapidly, reaching its normal water level of 825 m on October 24, and is ultimately maintained at approximately 824 m. The planar displacement data of 8 representative GNSS sites between November 2021 and November 2022 are illustrated in Fig. 8.

As shown in Fig. 8, the accumulative horizontal displacements of GNSS sites were about 48.7–107.2 mm before October 12, 2022, and the average displacement velocity is 84.6 mm/year. Based on the landslide velocity classification proposed by Cruden (1996), the TDG landslide is considered to be at the stage of slow deformation. However, the landslide displacement is extremely enlarged since the reservoir level has been impounded to 810 m. This indicates that the reservoir filling has reactivated the TDG landslide. The GNSS3 had the largest cumulative horizontal displacement of 758.65 mm by November 30, 2022, and its average displacement rate reached 13.29 mm/day in the last 49 days.

A borehole inclinometer is the most direct way to understand the landslide deformation near slide surface and identify the slip zone (Song et al. 2018). Figure 9 shows the deep displacement data measured by four inclinometers installed in the boreholes. As shown in Fig. 9b, the cumulative displacement value of IN-2 was mainly negative. Through a complete understanding of the site situation and analyzing the cause of the instrument failure, it was found that the instrument probe had been damaged. It can be seen that the cumulative displacements of inclinometers IN-1, IN-3, and IN-4 have been increasing during the monitoring period, indicating that the landslide deformation is still ongoing. In addition, all inclinometers showed obvious shear displacement at different depths, as shown in Fig. 9. The depth of the slip zone is 30.5 m in borehole IN-1, 88.5 m in borehole IN-3, and 69.5 m in borehole IN-4. From October 10, 2022, to October 26, 2022, the slip surface at 30.5 m of IN-1 moved at a rate of 0.14 mm/d to 2.96 mm/d, indicating that the deformation was accelerated by reservoir filling.

The failure mechanism of Tuandigou landslide and discussion

Understanding the deformation mechanism of TDG landslide is an important premise for evaluating its stability and providing an early warning of the landslide. The displacement monitoring data in Fig. 8 suggest that rainfall is rare during reservoir impounding and thus may not induce fast deformation of the TDG landslide. Therefore, of reservoir water level and lithology factors are selected for comprehensive analysis.

Correlation of landslide deformation with reservoir impounding

The Pearson cross-correlation coefficient (PCC) is adopted in this study to quantify the correlation between the horizontal displacement measured by GNSS stations and reservoir water level. The

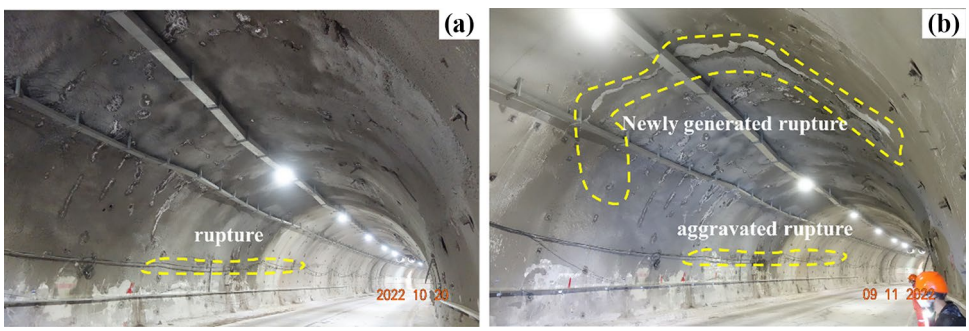

Fig. 7 Photos of concrete cracking in the K8 + 486-K8 + 548 m section of the DWZ tunnel

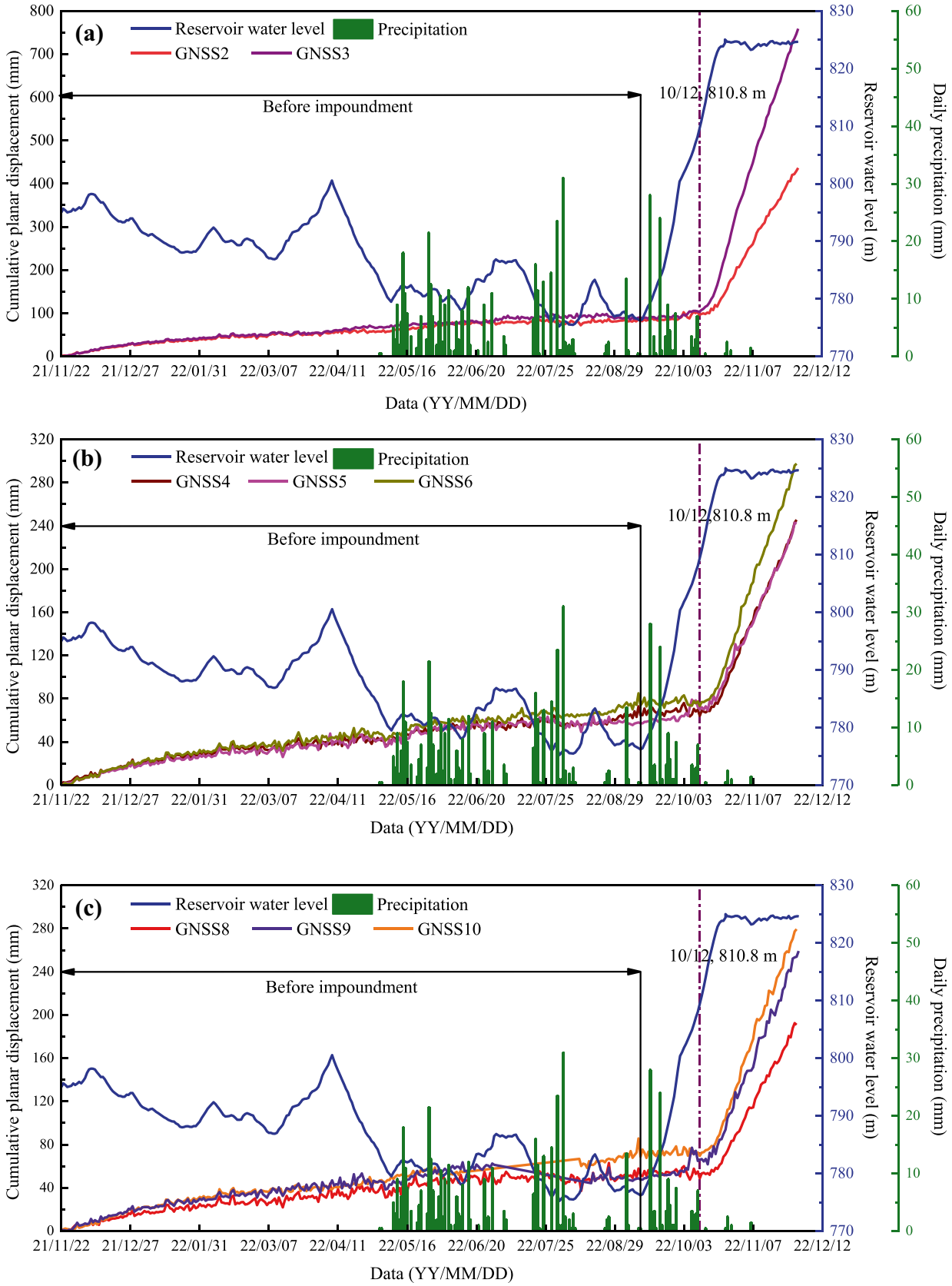

Fig. 8 Cumulative planar displacements, reservoir water levels, and rainfall of Tuandigou landslide. **a** GNSS2 and GNSS3; **b** GNSS4, GNSS5, and GNSS6; **c** GNSS8, GNSS9, and GNSS10

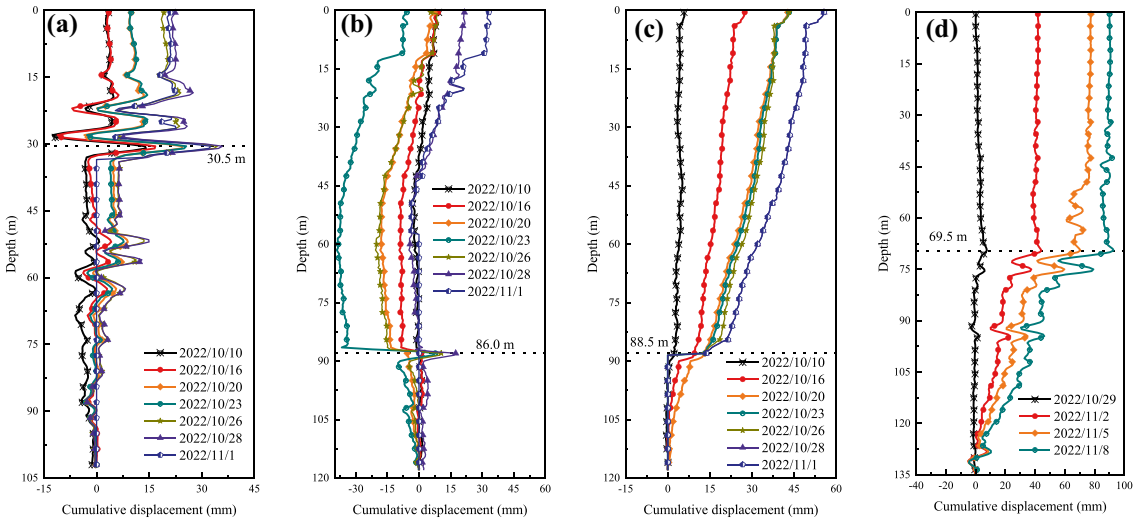

Fig. 9 In-depth displacement measured by the borehole inclinometers. **a** Displacement curve of IN-1, **b** displacement curve of IN-2, **c** displacement curve of IN-3, and **d** displacement curve of IN-4

formula of PCC is expressed as (Huang et al. 2020; Xu and Niu 2018; Zhang et al. 2023):

$$R_{xy} = \frac{\sum_{i=1}^{n}(x_i - \bar{x})(y_i - \bar{y})}{\sqrt{\sum_{i=1}^{n}(x_i - \bar{x})^2}\sqrt{\sum_{i=1}^{n}(y_i - \bar{y})^2}} \quad (1)$$

where R_{xy} is the correlation coefficient. x_i and y_i represent the value of reservoir water level and horizontal displacement of the TDG landslide at the i^{th} location, respectively. $\bar{x}$ is the mean value of reservoir water level, and $\bar{y}$ expresses the mean value of the horizontal displacement.

The value of $|R_{xy}|$ ranges from 0 to 1, and the greater the value of $|R_{xy}|$, the stronger the correlation between the reservoir water level and landslide deformation. Besides, the index of significance level *Sig* is also calculated to identify the statistical correlation between two random variables *X* and *Y*. If *Sig* is less than 0.05, there is a significant statistical correlation between the two variables.

Table 2 shows the results of the PCC analysis between horizontal displacement and reservoir water level. As illustrated in Table 2, the values of correlation coefficient R_{xy} for all the selected GNSS stations are between 0.5 and 0.8. Based on the study of Xu et al. (2021), the degree of correlation between landslide deformation and reservoir water level is moderate. Furthermore, the *Sig* for all GNSS stations is equal to zero, indicating that a significant statistical correlation between the reservoir water level and landslide deformation.

Figure 10 illustrates the horizontal displacement rate of GNSS2 and GNSS3 and its relationship with reservoir water level and rainfall. It can be found that the displacement rate accelerates during the period of reservoir filling from 810 to 825 m. The peak displacement rate of GNSS2 and GNSS3 is 15.3 mm/day and 18.7 mm/day, respectively. The results indicate that deformation velocity is closely related to the reservoir impounding, but no to rainfall. In other words, the reactivation of TDG landslide is mainly controlled by the filling of the reservoir.

Correlation of landslide deformation with lithologic factors

As mentioned in Section "Material compositions and structure characteristics", there are three main strata from the old to the new in the TDG landslide. Among them, the Xiwangmiao Formation (Є2x) distributes on steep slopes with elevation ranging from 700 to 1300 m. Moreover, the upper layer of Є2x is soft-hard integrated, consisting of purplish red, gray-green extra-thin sandstone, and silty mudstone, locally interbedded with gypsum. Under the effect of river erosion and bank slope unloading, the medium-thick dolomite in the front edge of the landslide becomes thinner. It gradually loses its supporting role, making the rock mass at the front edge of the landslide collapse and the trailing edge slip.

As shown in Fig. 11, the slip deformation of the gypsum interlayer along the top of $Є_2x_1$ occurs at the upstream side boundary of the TDG landslide with an elevation of 1030 m. After the reservoir impounding, the water level rises rapidly, aggravating the erosive effects of the buckling bank slope. Therefore, the rock mass at the

Table 2 Correlation between horizontal displacement and reservoir water level

GNSS station	Person cross-correlation coefficient	Significance
GNSS2	0.676	0.000
GNSS3	0.710	0.000
GNSS4	0.625	0.000
GNSS5	0.640	0.000
GNSS6	0.641	0.000
GNSS8	0.583	0.000
GNSS9	0.695	0.000
GNSS10	0.670	0.000

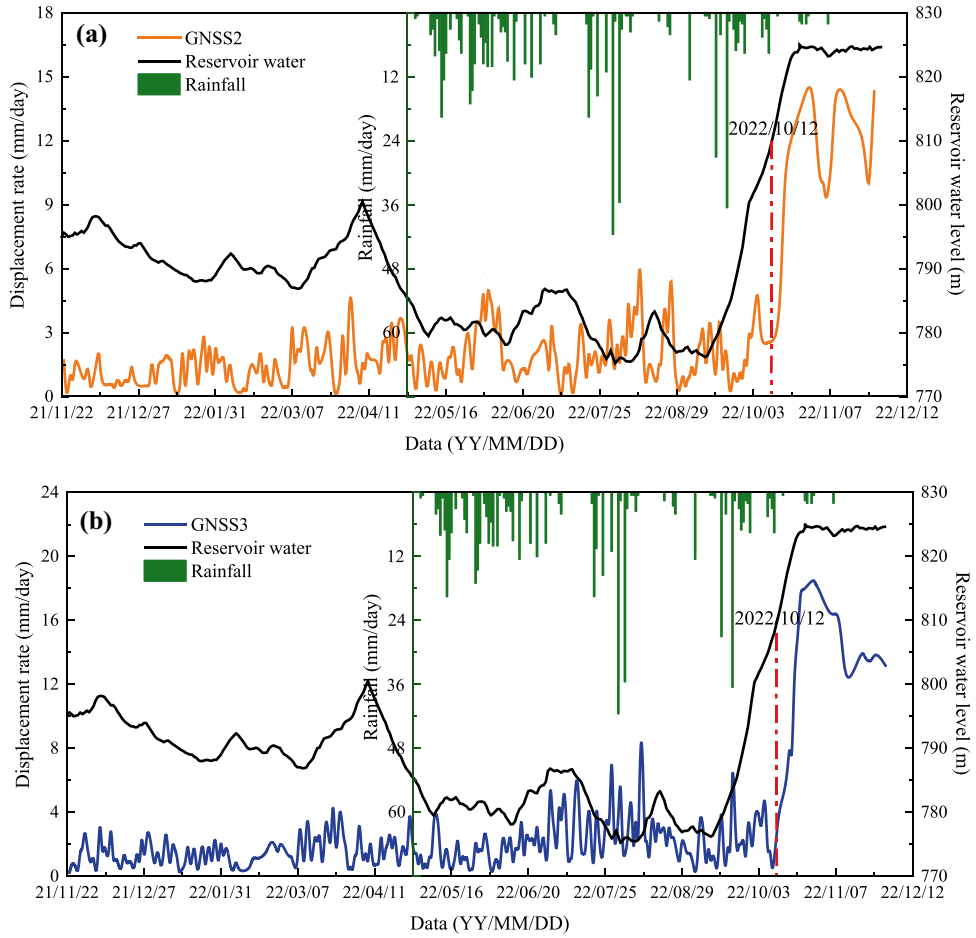

Fig. 10 Variations of horizontal displacement rate due to reservoir water level fluctuation and rainfall. **a** Displacement rate of GNSS2 and **b** displacement rate of GNSS3

front edge of the landslide is left unsupported and the deformation process of the slope occurs. The rock mass within the landslide is transformed from dry/unsaturated to saturated, decreasing the rock strength due to water-induced weakening and breaking the limit equilibrium state of the bank slope. In other words, reservoir impounding has reactivated the ancient TDG landslide.

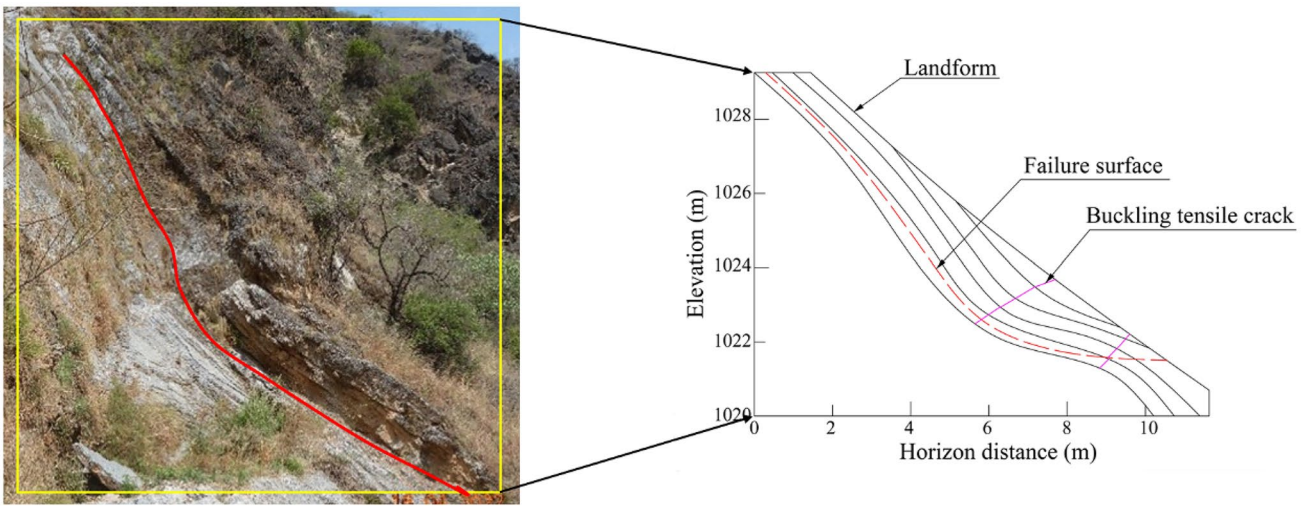

Fig. 11 Twisted shear micro-geomorphology of upper steep rock stratum in 8# gully

Conclusions

This paper reports detailed deformation characteristics of the TDG landslide in the Baihetan reservoir area based on field investigation and in-situ monitoring. Subsequently, the triggering mechanism of the TDG landslide is analyzed and discussed. It is found that the landslide deformation is closely related to the reservoir water level. The TDG landslide was in a slow deformation stage before the reservoir filling. After the reservoir water level reached the elevation of 810 m, the ground cracks continued to expand and gradually linked up, resulting in an accelerated deformation of the TDG landslide. At this stage, the deformation DWZ tunnel in the section of K8 + 486–K8 + 548 m was also intensified, including concrete cracking and local blocking. Furthermore, the lithology in the study area also has a positive contribution to the slide movement.

Based on the water level operation plans of Baihetan reservoir, the water level will gradually drop to 765 m. During the drawdown period, the influence of rock mass permeability coefficient usually makes the change rate of groundwater within the landslide and reservoir water level different. Consequently, the hydrodynamic pressure in the landslide gradually generates and may induce the overall sliding of the TDG landslide. Therefore, early warning and control of the TDG landslide should be strengthened during the drawdown period of the Baihetan reservoir.

Acknowledgements

The authors wish to acknowledge Xuewen Fan and Qi Li from Zhejiang Huadong Construction Engineering Corporation Limited for providing the monitoring data. In addition, the authors are very grateful for the constructive comments of the viewers, which significantly improved the quality of the manuscript.

Funding

The work presented in this paper is supported by the Key Science and Technology Plan Project of PowerChina Huadong Engineering Corporation Limited (Grant No. KY2021-ZD-03).

Data availability

The data that support the findings of this study are available on request from the corresponding author, Shiqi Liu. The data are not publicly available due to restrictions.

Declarations

Conflict of interest The authors declare no competing interest.

References

Barla G, Paronuzzi P (2013) The 1963 Vajont landslide: 50th anniversary. Rock Mech Rock Eng 46(6):1267–1270. https://doi.org/10.1007/s00603-013-0483-7

Crosta GB, Imposimato S, Roddeman D (2015) Landslide spreading, impulse water waves and modelling of the Vajont rockslide. Rock Mech Rock Eng 49(6):2413–2436. https://doi.org/10.1007/s00603-015-0769-z

Cruden DM (1996) Landslide types and processes. Special Report, National Research Council, Transportation Research Board 247:36–76

Dun J, Feng W, Yi X et al (2021) Detection and mapping of active landslides before impoundment in the Baihetan reservoir area (China) based on the time-series InSAR method. Remote Sens 13(16). https://doi.org/10.3390/rs13163213

Huang B, Yin Y, Du C (2016) Risk management study on impulse waves generated by Hongyanzi landslide in Three Gorges Reservoir of China on June 24, 2015. Landslides 13(3):603–616. https://doi.org/10.1007/s10346-016-0702-x

Huang D, Luo S-L, Zhong Z et al (2020) Analysis and modeling of the combined effects of hydrological factors on a reservoir bank slope in the Three Gorges Reservoir area, China. Eng Geol 279. https://doi.org/10.1016/j.enggeo.2020.105858

Ibañez JP, Hatzor YH (2018) Rapid sliding and friction degradation: lessons from the catastrophic Vajont landslide. Eng Geol 244:96–106. https://doi.org/10.1016/j.enggeo.2018.07.029

Kilburn CRJ, Petley DN (2003) Forecasting giant, catastrophic slope collapse: lessons from Vajont, Northern Italy. Geomorphology 54(1–2):21–32. https://doi.org/10.1016/s0169-555x(03)00052-7

Liu H, Luo Y, Feng W et al (2023) Site response of ancient landslides to initial impoundment of Baihetan reservoir (China) based on ambient noise investigation. Soil Dyn Earthq Eng 164. https://doi.org/10.1016/j.soildyn.2022.107590

Paronuzzi P, Rigo E, Bolla A (2013) Influence of filling–drawdown cycles of the Vajont reservoir on Mt. Toc slope stability. Geomorphology 191:75–93. https://doi.org/10.1016/j.geomorph.2013.03.004

Song K, Wang F, Yi Q et al (2018) Landslide deformation behavior influenced by water level fluctuations of the Three Gorges Reservoir (China). Eng Geol 247:58–68. https://doi.org/10.1016/j.enggeo.2018.10.020

Tang H, Wasowski J, Juang CH (2019) Geohazards in the three Gorges Reservoir Area, China – lessons learned from decades of research. Eng Geol 261. https://doi.org/10.1016/j.enggeo.2019.105267

Tang H, Yong R, Ez Eldin MAM (2016) Stability analysis of stratified rock slopes with spatially variable strength parameters: the case of Qianjiangping landslide. Bull Eng Geol Env 76(3):839–853. https://doi.org/10.1007/s10064-016-0876-4

Wang F, Zhang Y, Huo Z et al (2008) Mechanism for the rapid motion of the Qianjiangping landslide during reactivation by the first impoundment of the Three Gorges Dam reservoir, China. Landslides 5(4):379–386. https://doi.org/10.1007/s10346-008-0130-7

Wang F-W, Zhang Y-M, Huo Z-T et al (2004) The July 14, 2003 Qianjiangping landslide, Three Gorges Reservoir, China. Landslides 1(2). https://doi.org/10.1007/s10346-004-0020-6

Wolter A, Stead D, Ward BC et al (2015) Engineering geomorphological characterisation of the Vajont Slide, Italy, and a new interpretation of the chronology and evolution of the landslide. Landslides 13(5):1067–1081. https://doi.org/10.1007/s10346-015-0668-0

Wu H, Nian T-K, Shan Z-G et al (2023) Rapid prediction models for 3D geometry of landslide dam considering the damming process. J Mt Sci 20:1–15. https://doi.org/10.1007/s11629-022-7906-z

Wu S, Hu X, Zheng W et al (2022) Displacement behaviour and potential impulse waves of the Gapa landslide subjected to the Jinping reservoir fluctuations in Southwest China. Geomorphology 397. https://doi.org/10.1016/j.geomorph.2021.108013

Xu Q, Zhang T, Chen J et al (2021) The influence of reinforcement strengthening on seismic response and index correlation for high arch dams by endurance time analysis method. Structures 32:355–379. https://doi.org/10.1016/j.istruc.2021.03.007

Xu S, Niu R (2018) Displacement prediction of Baijiabao landslide based on empirical mode decomposition and long short-term memory neural network in Three Gorges Area, China. Comput Geosci 111:87–96. https://doi.org/10.1016/j.cageo.2017.10.013

Yan L, Xu W, Wang H et al (2019) Drainage controls on the Donglingxing landslide (China) induced by rainfall and fluctuation in reservoir water levels. Landslides 16(8):1583–1593. https://doi.org/10.1007/s10346-019-01202-x

Yi X, Feng W, Wu M et al (2022) The initial impoundment of the Baihetan reservoir region (China) exacerbated the deformation of the Wangjiashan landslide: characteristics and mechanism. Landslides 19(8):1897–1912. https://doi.org/10.1007/s10346-022-01898-4

Yin Y, Huang B, Wang W et al (2016) Reservoir-induced landslides and risk control in Three Gorges Project on Yangtze River, China. J Rock

Mech Geotech Eng 8(5):577–595. https://doi.org/10.1016/j.jrmge.2016.08.001
Yin Y-P, Huang B, Chen X et al (2015) Numerical analysis on wave generated by the Qianjiangping landslide in Three Gorges Reservoir. China Landslides 12(2):355–364. https://doi.org/10.1007/s10346-015-0564-7
Zhang C, Yin Y, Yan H et al (2021) Reactivation characteristics and hydrological inducing factors of a massive ancient landslide in the Three Gorges Reservoir, China. Eng Geol 292. https://doi.org/10.1016/j.enggeo.2021.106273
Zhang T, Xu Q, Chen J et al (2023) Nonlinear seismic response and index correlation of high arch dams under cross-stream oblique incidence of near-fault SV waves based on wavelet decomposition. Soil Dyn Earthq Eng 164. https://doi.org/10.1016/j.soildyn.2022.107635
Zhou C, Cao Y, Yin K et al (2022) Characteristic comparison of seepage-driven and buoyancy-driven landslides in Three Gorges Reservoir area, China. Eng Geol 301. https://doi.org/10.1016/j.enggeo.2022.106590

Zhichao Cheng · Shiqi Liu (✉) · Anchi Shi
PowerChina Huadong Engineering Corporation Limited, Hangzhou 311122, China
Email: sddxlsq@126.com

Zhichao Cheng · Xuewen Fan
Zhejiang Huadong Construction Engineering Corporation Limited, Hangzhou 310030, China

Kexin Yin
Department of Civil and Airport Engineering, Nanjing University of Aeronautics and Astronautics, Nanjing 211106, China